

# Thermal evolution of massive compact objects with dense quark cores

Daniel Hess, Armen Sedrakian

*Institute for Theoretical Physics, J.-W. Goethe University, D-60438 Frankfurt-Main, Germany*

(Dated: November 10, 2018)

We examine the thermal evolution of a sequence of compact objects containing low-mass hadronic and high-mass quark-hadronic stars constructed from a microscopically motivated equation of state. The dependence of the cooling tracks in the temperature versus age plane is studied on the variations of the gaplessness parameter (the ratio of the pairing gap for red-green quarks to the electron chemical potential) and the magnitude of blue quark gap. The pairing in the red-green channel is modeled assuming an inhomogeneous superconducting phase to avoid tachionic instabilities and anomalies in the specific heat; the blue colored condensate is modeled as a Bardeen-Cooper-Schrieffer (BCS)-type color superconductor. We find that massive stars containing quark matter cool faster in the neutrino-cooling era if one of the colors (blue) is unpaired and/or the remaining colors (red-green) are paired in a inhomogeneous gapless superconducting state. The cooling curves show significant variations along the sequence, as the mass (or the central density) of the models is varied. This feature provides a handle for fine-tuning the models to fit the data on the surface temperatures of same-age neutron stars. In the late-time photon cooling era we observe inversion in the temperature arrangement of models, *i.e.*, stars experiencing fast neutrino cooling are asymptotically hotter than their slowly cooling counterparts.

## I. INTRODUCTION

After the initial phase of rapid (of order of days to weeks) cooling from temperatures  $T \sim 50$  MeV down to 0.1 MeV, a neutron star settles in a thermal quasiequilibrium state which evolves slowly over the time scales  $10^3 - 10^5$  yr down to temperatures  $T \sim 0.01$  MeV. The cooling rate of the star during this period is determined by the processes of neutrino emission from dense matter, whereby the neutrinos, once produced, leave the star without further interactions. The understanding of the cooling processes that take place during this neutrino radiation era is crucial for the interpretation of the data on surface temperatures of neutron stars. While the long term features of the thermal evolution of neutron stars are insensitive to the initial rapid cooling stage ( $t \leq$  years), the subsequent route in the temperature versus time plane, which includes in addition to the neutrino emission era the late-time ( $t \geq 10^5$  yr) photoemission era, strongly depends on the emissivity of matter during the neutrino-cooling era [1–4].

The neutrino emission during the neutrino-cooling era chiefly originates from the core of a compact object, *i.e.*, from matter at and above densities  $\sim 0.16$  fm $^{-3}$  and is sensitive to its composition. Hadronic matter emits neutrinos mainly via the beta and inverse beta decay processes and the charge neutral processes of Cooper pair breaking. The former are suppressed by pairing correlations (*i.e.*, the emergence of a gap in the quasiparticle spectrum separating the ground state from the excited states below certain critical temperature), whereas the latter are the consequence of the formation of Cooper pair condensates [4].

The densities in the centers of massive compact objects can be by an order magnitude greater than the nuclear saturation density. The quark substructure of the baryons will play an increasingly important role as

larger densities are reached in progressively massive objects. The recent timing observations of binary millisecond pulsar J1614-2230 imply that compact objects with masses of order of 2 solar masses exist in nature [5].

It is the purpose of this work to examine the cooling behavior of massive compact objects containing cores of deconfined interacting quark matter. Specifically, we shall assume that above certain density the quarks are in continuum states filling a Fermi sphere. The mechanism by which the neutrinos are produced in quark matter are basically the same as in the baryonic matter, *i.e.*, beta decays of  $d$  quarks and inverse beta decays via electron capture on a  $u$  quark. Because of our assumption of filled Fermi spheres and attractive interaction among quarks in dominant color antisymmetric states, the pairing of quarks - known as color superconductivity - needs to be taken into account [6–12]. In this paper, we shall concentrate on simple  $ud$ -quark condensates and explore the possibility that these condensates are in one of the gapless phases with broken spatial symmetry [13–21]. The homogeneous gapless color superconductors are not treated because they develop tachionic instabilities in the ground state [22] and their specific heat has anomalous temperature dependence [23].

Thermal components in the photon spectra from a handful of pulsars have been identified. The temperatures inferred from these measurements point toward a dichotomy in the evolution of isolated neutron stars - some of them are clearly much hotter than their same-age counterparts. The scatter in the data over the temperature-age plane could be correlated with certain static (mass, radius) and/or dynamic (spin,  $B$ -field) parameter(s) of pulsars. Such correlations are not easy to resolve theoretically, as there could be a number of factors influencing the emitted spectrum (*e.g.*, the properties of the emitting regions could be sensitive to the variation of the magnetic fields at the surface of the star

and its composition).

One of the aims of this work is to understand the correlation between the mass and the surface temperature of a cooling compact object for a class of models which support high-mass ( $M \sim 2M_\odot$ ) stars. Specifically, we shall study below the models constructed in Ref. [24]. The sequences of static and rotating configurations of Ref. [24] have maximal masses of the order  $2M_\odot$  with radii of the order of 12 km. The internal structure of these models is described in Ref. [25], where it is shown that their massive members contain quark cores with radii of the order of 7 km and masses  $\leq 1M_\odot$ .

Previous work studied the cooling of quark-hadronic stars with different input physics and varying degree of realism. From simulations of cooling of compact stars with a mixed phase of quarks and hadrons, in which the neutrino emission processes are uniformly suppressed by a gap in quark spectrum, one may conclude that quark matter is invisible if the gap in quark matter is large and indistinguishable from hadronic matter if the gap is small [26]. In simulations of the cooling compact objects of  $1.4 M_\odot$  with quark cores in the color-flavor-locked (CFL) phase, the cooling is too fast to accommodate the observational data [27]. Because all the fermions in the CFL phase are gapped, the quark core remains hot for longer periods of time (up to 100 yr) compared to the phases containing ungapped fermions in the quark phase. The cooling simulations of Ref. [28] of  $1.4 M_\odot$  toy models having core quark matter in the gapless version of the CFL phase show that the cores of such stars would be much hotter than their nuclear counterparts in the photon cooling era. This is because such matter has larger specific heat due to quadratic rather than linear dependence of the quasiparticle spectrum on the momentum. The thermal behavior of Larkin-Ovchinnikov-Fulde-Ferrell quark matter was studied for  $1.4 M_\odot$  toy models, and it was concluded that such phases will lead to rapid cooling of compact stars with rates that are comparable to the rate found for the unpaired quark matter [29]. The quark stars that contain two-flavor quark matter in a homogeneous state, possibly in a mixed state with normal quark matter, would cool too fast to account for the data [30]. The possibility that the normal quarks additionally pair in some channel fits the data [30, 31] if the masses of the models are varied in a range  $1.0 - 1.75 M_\odot$  and some suitable density dependence is assigned to the smaller gap.

In this work, we are concerned with the thermal evolution of a sequence of compact objects, parametrized by their central density or mass, which contains large-mass ( $M \leq 2M_\odot$ ) members with quark cores. Our models have realistic backgrounds, being derived from a microscopically motivated equation of state and the general relativistic structure equations. One aim of this study is to quantify the changes in the cooling behavior of stars along the sequence, focusing mainly on the new features that arise with the onset of quark matter in the cores of high-mass models. We assume quark matter of light

$u$  and  $d$  quarks in beta equilibrium with electrons; the  $s$  and other quark flavors are suppressed by their large masses. The pairing among the  $u$  and  $d$  quarks occurs in two channels: the red-green quarks are paired in a condensate with gaps of the order of the electron chemical potential; the blue quarks are paired with (smaller) gaps of order of keV, which is comparable to core temperature during the neutrino-cooling epoch [32–34]. The neutrino emission in the case of single-flavor, but multicolor pairing is as in normal quark matter [35] and differs from the single-color case studied here.

A homogenous red-green condensate, when in the gapless BCS regime, develops tachionic instabilities, which manifest themselves in negative Meissner masses [22]. Furthermore, the thermodynamic quantities of a homogeneous gapless superconductor are generally anomalous at low temperatures; in particular, for large enough asymmetries the gap disappears at a lower critical temperature and the specific heat experiences a jump [19, 23]. Recent studies show that a realization of inhomogeneous superconductors, the Fulde-Ferrell phase, is preferred in color superconducting quark matter to the homogenous BCS phase at sufficiently low temperature and weak coupling for arbitrary flavor asymmetries [20] as well as when color and charge neutrality are enforced [21]. Furthermore, the anomalies in the thermodynamic quantities are cured when the inhomogeneous phases are treated (this conjecture is rigorously proven for the so-called Fulde-Ferrell phase [19–21]).

Motivated by these observations and to avoid anomalies related to the homogeneous phases, we shall assume a generic inhomogeneous state and model the neutrino emission and specific heat in a phenomenological manner (see Sec. II). For the red-green condensate, we shall use a parameterization of neutrino emissivity in terms of the gaplessness parameter, as proposed in Ref. [36]. Thus, the second aim of this work is to understand the systematics of the cooling tracks in the temperature versus age plane when the “gaplessness” parameter, *i.e.*, the ratio of the pairing gap for red-green quarks to the electron chemical potential is varied. The magnitude of the gap in the spectrum of blue quarks is another parameter that will be varied. We do not attempt to fit the data by fine-tuning the available parameters (the mass of the star, the gaplessness parameter, and the gap for blue quarks); rather, we would like to find general trends that could provide orientation once the observational data demands such fits.

This article is organized as follows. In Sec. II, we describe the models of purely hadronic and quark-hadronic stars, the pairing patterns in quark matter, and the microscopic input needed for studying their thermal evolution. Section III studies the thermal evolution of these models. Here, we discuss the key approximations used to evolve the models in time and discuss the variations in cooling behavior as the central density of the models as well as the pairing parameters are changed. Our conclusions are collected in Sec. IV. Some preliminary results

were reported in Refs. [37–39].

## II. QUARK CORES AND NEUTRINO EMISSION PROCESSES

### A. Equation of state, composition, and pairing

We start with a brief description of the models underlying our study. The low-density nuclear matter equation of state is based on a relativistic model of nuclear matter in a homogeneous core and an inhomogeneous low-density phase constituting the crust of the star (see Ref. [24] for details). The high-density matter equation of state is derived from the effective Nambu-Jona-Lasinio four-fermion interaction model which incorporates the pairing interactions among quarks. The two equations were matched by a Maxwell construction, *i.e.*, the requirement that the pressures of the two phases at the point of transition to the deconfined quark phase should match at a fixed baryo-chemical potential. The high-density quark phase pairs the up ( $u$ ) and down ( $d$ ) quarks. We will assume that strange quarks (because of their large mass) are not important at the densities relevant to our models. With this equation of state as an input, the models of low-density purely hadronic and high-density quark-hadronic stars were constructed by solving the general relativistic structure equations. The masses and radii of various components are shown for a set of models in Table I. It is assumed that the transition from the hadronic core to the crust occurs at  $0.5\rho_0$ , where  $\rho_0 = 2.8 \times 10^{14} \text{ g cm}^{-3}$  is the nuclear saturation density. In the isothermal-interior approximation described below, the temperature gradients are concentrated in the envelope of the star; the transition from isothermal interior to the nonisothermal envelope occurs at the density  $\rho_m = 10^{10} \text{ g cm}^{-3}$  and the radius  $R_{cr}$ . Table I lists the values of the inner radius  $R_{cr}$  of the models.

Figure 1 shows the density profiles of four models selected from the set above, whose thermal evolution will be studied in Sec. III. One of these is a purely hadronic model with central density  $\rho_{c,14} = 5.1$ , where  $\rho_{c,14} = \rho_c/(10^{14} \text{ g cm}^{-3})$ . The remaining three models contain a quark matter core and have central densities  $\rho_{c,14} = 10.8, 11.8, 21.0$ . The model with  $\rho_{c,14} = 21.0$  has the maximum mass for the sequence of the stars defined by the equation of state above, *i.e.*, for larger central densities the stable branch of equilibrium, nonrotating, configurations terminates. The quark-hadron transition is seen in the density jump at the radius at which the phase transition occurs. (Note that the pressure and the baryonic chemical potential are continuous at the point of transition by construction.) The chosen models provide a good coverage of the possibilities provided by the underlying equation of state. In particular, a substantial fraction of the mass and volume of the model with largest central density is occupied by quark matter.

The combination of charge neutrality and beta equi-

TABLE I: Masses and the radii of models constructed from the equation of state adopted in this work. The low-density models are purely hadronic, whereas the high-density models contain quark cores. The central densities of the models are given in units of  $10^{14} \text{ g cm}^{-3}$ , the radii in kilometers, and the masses in units of the solar mass. The columns from left to right are: the central density, the radius of the quark core, the quark-plus-hadronic core, the isothermal interior and the star, the masses of the quark core, the hadronic core, the crust, and the star.

$\rho_{c,14}$	$R_Q$	$R_{Q+H}$	$R_{cr}$	$R$	$M_Q$	$M_H$	$M_{cr}$	$M$
3.6	-	9.48	13.20	13.80	-	0.43	0.11	0.54
5.1	-	11.47	13.39	13.53	-	1.03	0.07	1.10
8.2	-	12.57	13.55	13.57	-	1.81	0.04	1.85
10.8	0.68	12.54	13.49	13.5	0.001	1.81	0.040	1.91
11.8	3.41	12.40	13.31	13.32	0.09	1.80	0.04	1.93
15.0	5.84	11.86	12.54	12.55	0.52	1.46	0.03	2.01
21.0	6.77	11.34	11.91	11.92	0.89	1.14	0.02	2.05

librium implies the presence in the stellar matter of electrons, whose chemical potential obeys the condition  $\mu_e = \mu_d - \mu_u$ . Because of the shift in the chemical potentials of the quarks of different flavors, the pairing pattern differs from the conventional Bardeen-Cooper-Schrieffer (BCS) superconductors by the fact that the paired fermions are drawn from different Fermi surfaces. Under these conditions the pairing is “gapless.” *i.e.*, there exist segments on the Fermi surface where the gap separating the excited states of the system from the ground state disappears. The gapless phases could be either homogeneous (in the sense that the spatial  $O(3)$  symmetry is intact) or inhomogeneous, in which case the symmetry is broken down to a certain symmetry subgroup.

### B. Neutrino emissivities and other input

Quark matter consisting of two light flavors cools via the beta decay (Urca) reactions

$$d \rightarrow u + e + \bar{\nu}, \quad u + e \rightarrow d + \nu, \quad (1)$$

where  $\nu$  and  $\bar{\nu}$  stand for neutrino and antineutrino. For unpaired quarks and to leading order in the strong coupling constant  $\alpha_s$  the emissivity of the process *per quark color* is given by [40]

$$\epsilon_\beta = \frac{914}{945} \tilde{G}^2 p_d p_u p_e \alpha_s T^6, \quad (2)$$

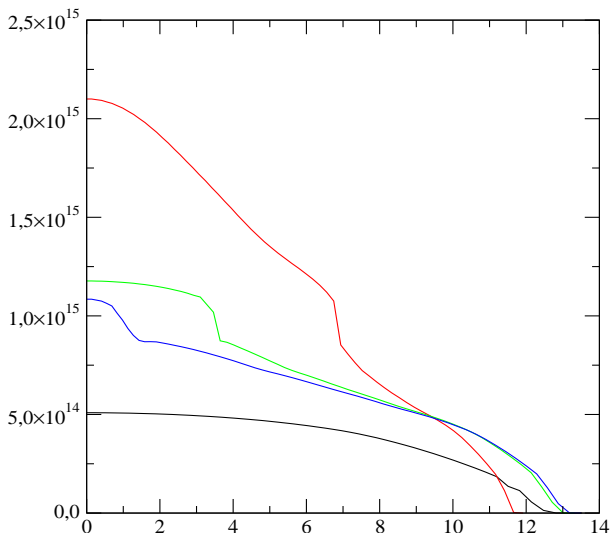


FIG. 1: Dependence of the density of the stellar matter on the radial coordinate for static, spherically symmetrical stars. The central densities and radii of the stars can be read off from the respective axes. The observed jumps in the density profiles of high-mass stars are a consequence of the onset of the quark matter in the core.

where  $\tilde{G} = G \cos \theta$  is the weak coupling constant,  $\theta$  is the Cabibbo angle,  $p_d$ ,  $p_u$ , and  $p_e$  are the Fermi momenta of down quarks, up quarks, and electrons. Non-Fermi-liquid corrections to the Urca rate above [41] were neglected in our study.

The quark pairing modifies the temperature dependence of the process (2). In the BCS-type superconductors, the process is suppressed nearly linearly for  $T \simeq T_c$  and exponentially for  $T \ll T_c$ , where  $T_c$  is the critical temperature [42]. In gapless superconductors the emergence of the new scale  $\delta\mu = (\mu_d - \mu_u)/2$  leads to two essentially different possibilities [36], which are distinguished by the value the dimensionless parameter  $\zeta = \Delta/\delta\mu$ , where  $\Delta$  is the gap in the spectrum in the limit  $\delta\mu = 0$ . When  $\zeta > 1$ , the entire Fermi surface is gapped, *i.e.*, when the thermal smearing of the Fermi surface  $\sim T$  is much smaller than the gap, no excitation can be created out of the Fermi sphere. In this respect, the  $\zeta > 1$  case resembles ordinary BCS superconductors. When  $\zeta < 1$ , particles can be excited from the gapless regions of the Fermi sphere. We shall use below the interpolation formula proposed in Ref. [36], which covers these asymptotic limits, *i.e.*,

$$\epsilon_{\beta}^{rg}(\zeta; T \leq T_c) = 2f(\zeta)\epsilon_{\beta}, \quad (3)$$

$$f(\zeta) = \frac{1}{\exp[(\zeta - 1)\frac{\delta\mu}{T} - 1] + 1},$$

where the factor two comes from the two colors of quarks involved in the pairing. Since the pairing pattern breaks the  $SU(3)$  color symmetry, one of the quark colors (say, blue) remains unpaired. Same-color pairing leads to

much smaller gaps in the spectrum of the quarks; these could be as small as tens of keV, and therefore irrelevant in the neutrino-cooling era where  $T > 100$  keV in the core. The pairing in this case is BCS-type, and we shall simply parameterize the modifications of the Urca process on blue quarks as in the case of baryonic matter, *i.e.*,

$$\epsilon_{\beta}^b(T \leq T_c) = \epsilon_{\beta} \exp\left(-\frac{\Delta_b}{T}\right). \quad (4)$$

Note that  $\epsilon_b^{\beta} = \epsilon_{rg}^{\beta}/2$  due to the different number of colors involved in these cases.

As in ordinary BCS superconductors, the pair correlations suppress the specific heat of quarks (for  $T \ll T_c$  exponentially); at  $T = T_c$ , the specific heat jumps (increases) if the phase transition to the superconducting phase is of second order. To model the modifications of the specific heat, we adopt the fitted formula for the ratio of the specific heat in the superconducting  $c_S$  and normal  $c_N$  phases [43]

$$\frac{c_S}{c_N}(\tau) = \begin{cases} (12\pi/\gamma)(2\gamma\tau)^{-3/2}e^{-\pi/(\gamma\tau)} & 0 \leq \tau \leq 0.3, \\ -0.244 + 0.255\tau + 2.431\tau^2 & 0.3 < \tau \leq 1, \end{cases} \quad (5)$$

where  $\tau = T/T_c$  is the temperature in units of the critical temperature and  $\gamma = 1.781$ . Equation (5) is applied to neutron, proton, and blue-quark condensates. Note that Eq. (5) applies strictly only to isotropic BCS condensates. The anisotropy of neutron  $P$ -wave condensate somewhat modifies this ratio [44].

For the inhomogeneous red-green condensate, one needs to rescale the critical temperature which changes with  $\delta\mu$ :

$$T_c(\zeta) \simeq T_{c0} \sqrt{1 - \frac{4\mu}{3\Delta_0}\delta(\zeta)}, \quad (6)$$

where  $\mu = (\mu_d + \mu_u)/2$ ,  $\Delta_0 = \Delta(\zeta = 0)$ ,  $T_{c0} = T_c(\zeta = 0)$ , and  $\delta(\zeta) = (n_d - n_u)/(n_d + n_u)$ . The fully gapped and gapless regimes behave differently; in the presence of gapless modes, the specific heat has a linear dependence on the temperature. A phenomenological way to model this behavior is given by the relation

$$c_S^{rg}(\zeta; T \leq T_c) = f(\zeta)c_N^{rg}, \quad (7)$$

where  $c_N^{rg}$  is the specific heat of red-green unpaired quarks, taken as that for noninteracting quarks [45] and  $c_S^{rg}$  is the specific heat of pair-correlated quarks. To compute the specific heat of the electrons, we assume they form a noninteracting, ultrarelativistic gas.

The hadronic matter in our models is composed of neutrons (constituting  $\sim 95\%$  of baryonic matter content), of protons (with abundances of  $\sim 5\%$  of baryonic matter) and electrons (whose number is equal to that of protons by virtue of charge neutrality). In the unpaired state, the dominant cooling agents for such

abundances are the modified Urca processes and neutral current bremsstrahlung processes, included in standard fashion. We use emissivities derived for the free pion-exchange model of strong interaction [46], but reduce them by a constant factor 5 to account for short-range repulsive component of the nuclear force. (Note that medium modifications of pion dispersion can further modify these rates and the resulting cooling substantially; see Ref. [47]. However, no clear evidence of such modification were found in experiments so far). The corresponding rates below  $T_c$  are exponentially suppressed, e.g., for the modified Urca process we have

$$\epsilon_{\beta \text{ mod}}(T \leq T_c) = \epsilon_{\beta \text{ mod}} \exp\left(-\frac{\Delta_n(T) + \Delta_p(T)}{T}\right). \quad (8)$$

In addition, we include the process of electron bremsstrahlung on nuclei in the crusts [48]. Following the latter reference, we assume that the ions form a fluid throughout the crust (or the number of impurities is high) so that the emissivity scales as  $T^6$ . If at some temperatures ions form a crystalline phase, the emissivities scale roughly as  $T^7$  (classical crystal) or as  $T^8$  (quantum crystal) and the bremsstrahlung emissivity is parametrically suppressed [49].

In the superfluid/superconducting hadronic phases, the processes of pair-breaking can contribute to the cooling [50]. The neutral vector current processes are strongly suppressed by multiloop processes [51–54], whereas the axial-vector emission can be taken at one-loop level to a good accuracy [50]. Therefore, only the axial-vector neutrino emission through the pair-breaking processes were included in the simulations. The density-dependent zero-temperature pairing gaps of neutrons and protons, that have been used in the simulations, are shown in Fig. 2. Their non-zero-temperature values can be obtained in terms of the zero-temperature values  $\Delta(0)$  using the formula [43]

$$\frac{\Delta(\tau)}{\Delta(0)} = \begin{cases} 1 - \sqrt{2\gamma\tau}e^{-\pi/(\gamma\tau)} & 0 \leq \tau \leq 0.5, \\ \sqrt{3.016(1-\tau) - 2.4(1-\tau)^2} & 0.5 < \tau \leq 1, \end{cases} \quad (9)$$

which reproduces the exact BCS result with an error of order of a percent.

### III. THERMAL EVOLUTION

Our models were evolved in time, with the input described above, to obtain the temperature evolution of the isothermal-interior. The isothermal-interior approximation is valid for timescales  $t \geq 100$  yr, which are required to dissolve temperature gradients by thermal conduction. Unless the initial temperature of the core is chosen too low, the cooling tracks exit the nonisothermal phase and settle at a temperature predicted by the balance of the dominant neutrino emission and the specific heat of the core *at the exit temperature*. The thermal conduction is

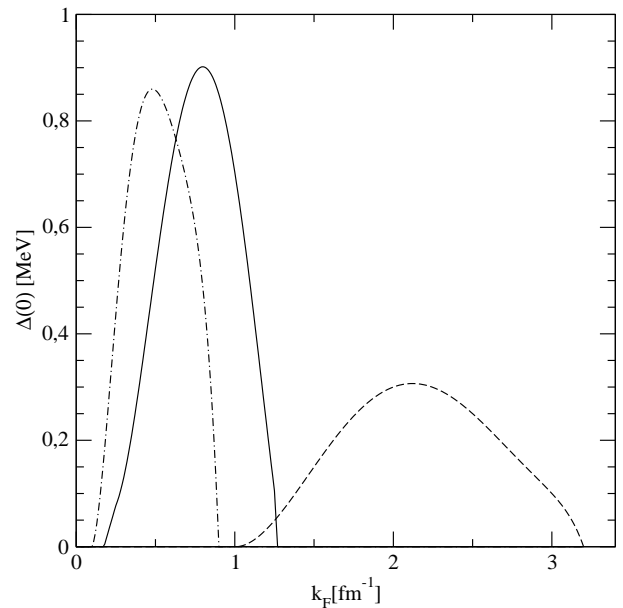


FIG. 2: Dependence of the neutron and proton pairing gaps on their Fermi momenta, (solid line -  ${}^1S_0$  neutron gap [62], dashed line -  ${}^3P_2 - {}^3F_2$  neutron gap [63], and dashed-dotted line -  ${}^1S_0$  proton pairing gap [64]).

effective enough to erase thermal gradients at densities larger than  $10^{10}$  g cm $^{-3}$ . The low-density envelope maintains substantial temperature gradients throughout the entire evolution; the temperature drops by about 2 orders of magnitude within this envelope. The isothermal-interior approximation relies further on the fact that the details of the temperature gradients within the envelope are unimportant if we are interested only in the surface temperature. Models of the envelopes predict the scaling  $T_s^4 = g_s h(T)$ , where  $g_s$  is the surface gravity, and  $h$  is some function which depends on  $T$ , the opacity of crustal material, and its equation of state. We shall use the fitted formula  $T_8 = 1.288(T_{s6}^4/g_{s14})^{0.455}$  [55]. (Note that this relation does not take into account either the potential strong magnetization of neutron star envelopes or the presence of light elements in their surface layers. The modifications due to these factors are discussed in Refs. [56, 57]).

In the isothermal-interior approximation, the parabolic differential equation for the temperature reduces to an ordinary differential equation,

$$C_V \frac{dT}{dt} = -L_\nu(T) - L_\gamma(T_s) + H(T), \quad (10)$$

where  $L_\nu$  and  $L_\gamma$  are the neutrino and photon luminosities,  $C_V$  is the specific heat of the core, and the heating processes, which could be important in the photon cooling era, are neglected, *i.e.*,  $H(T) = 0$  (see Refs. [58, 59] for a summary of these processes). The photon luminosity is given simply by the Stephan-Boltzmann law  $L_\gamma = 4\pi\sigma R^2 T_s^4$ , where  $\sigma$  is the Stephan-Boltzmann con-

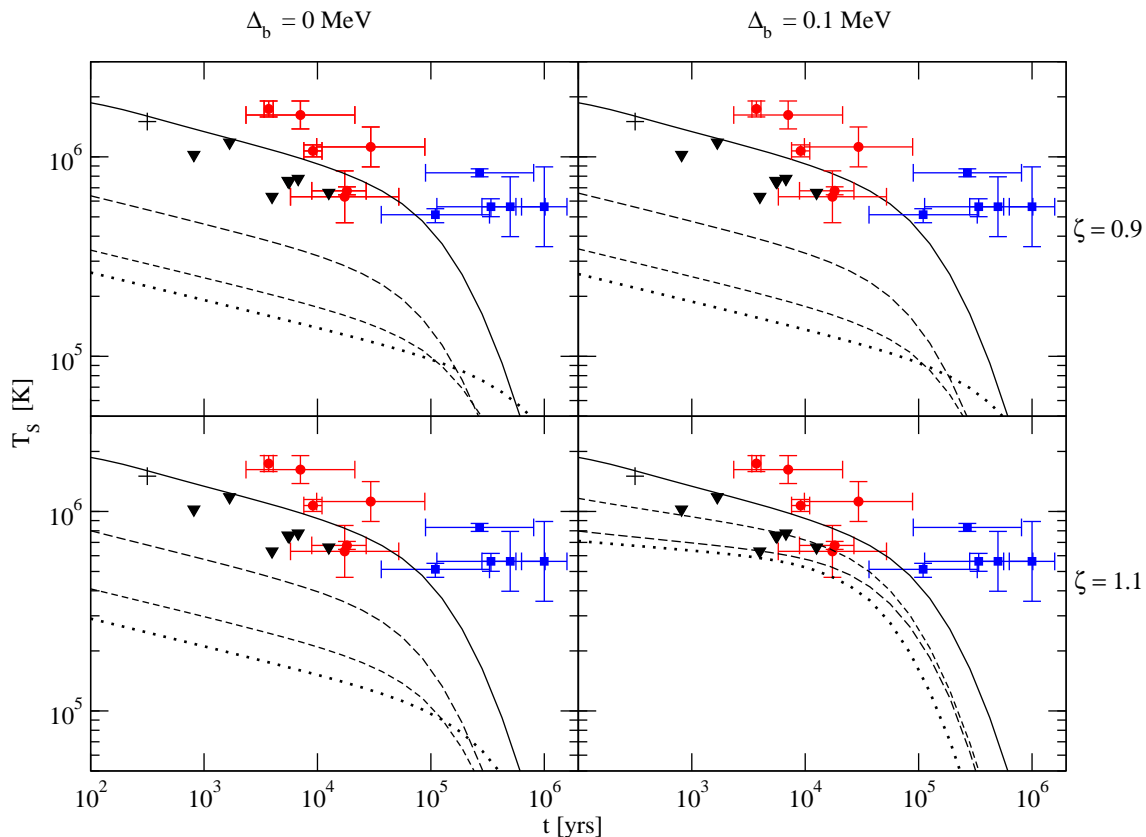


FIG. 3: Time evolution of the surface temperature of four models with central densities (in units of  $\rho_{14}$ ) 5.1 (solid line), 10.8 (long-dashed line), 11.8 (short-dashed line), 21.0 (dotted line). The integral parameters of these models can be found in Table I. The observational data points in order of increasing age correspond to RX J0822-4247, 1E 1207.4-5209, RX J0002+6246, PSR 1706-44, PSR 0833-45 (Vela), PSR 0538+2817 (dots, red online), PSR 0656+14, PSR 1055-52, PSR 0633+1748 (Geminga), RX J1856.5-3754, RX J0720.4-3125 (squares, blue online). The dots correspond to fits assuming H-atmospheres, squares – to black-body fits. The data is taken from Ref. [65]. The triangles show in order of increasing age the current upper limits on the surface temperatures of PSR J0205+6449 [66] PSR J112439.1-591620 [67], supernova remnants (SNRs) G093.3+6.9, G315.4-2.3, G084.2+0.8, and G127.1+0.5 [68], and RX J0007.0+73 [69]. The pulsar in Cas A is shown by the plus sign [60, 61]. The upper two panels correspond to cooling when the red-green condensate has  $\zeta = 0.9$ , *i.e.*, is not fully gapped; the lower panels correspond to  $\zeta = 1.1$ , *i.e.*, the red-green condensate is fully gapped. The left two panels correspond to evolution with negligible blue-quark pairing ( $\Delta_b = 0$ ); the right two panels show the evolution for large blue pairing  $\Delta_b = 0.1$  MeV.

stant. The neutrino luminosities  $L_\nu(T)$  and the specific heat  $C_V$  in Eq. (10) are spatial integrals of emissivities and local specific heats of constituents over the volume of the isothermal-interior. In nonsuperfluid matter, the temperature dependence of the luminosities and the specific heat in Eq. (10) can be factored out and the remaining coefficients need to be computed only once for a given stellar model. If matter is superfluid, the temperature *and* density dependence of the pairing gaps (or critical temperatures) cannot be factorized. Hence, we carry out the spatial integrations over the volume of the isothermal interior at each time step to obtain the relevant coefficients, which are now temperature dependent. Once the coefficients are known, Eq. (10) can be advanced in time, *e.g.*, through the Runge-Kutta algorithm. The results of integration of Eq. (10) are shown in Fig. 3, where we display the dependence of the (redshifted) sur-

face temperature on time. Each panel of Fig. 3 contains cooling tracks for the same set of four models introduced in Sec. III; the cooling tracks for the purely hadronic model (solid lines) are the same in all four panels. The panels differ in the values of microphysics parameters, which characterize the pairing pattern in quark matter. Specifically, the two panels in the left column correspond to the case where the blue-quark pairing is negligible (*i.e.*, the pairing is on a scale much smaller than the smallest energy scale involved, typically the core temperature). The two panels in the right column correspond to the case where the gap for blue quarks is large,  $\Delta_b = 0.1$  MeV. The panels in the upper and lower rows are distinguished by the value of the  $\zeta$  parameter. [We use the values  $\zeta = 0.9$  (upper row) and  $\zeta = 1.1$  (lower row)].

Figure 4 shows the dependence of the neutrino luminosities of contributing processes on the core temperature

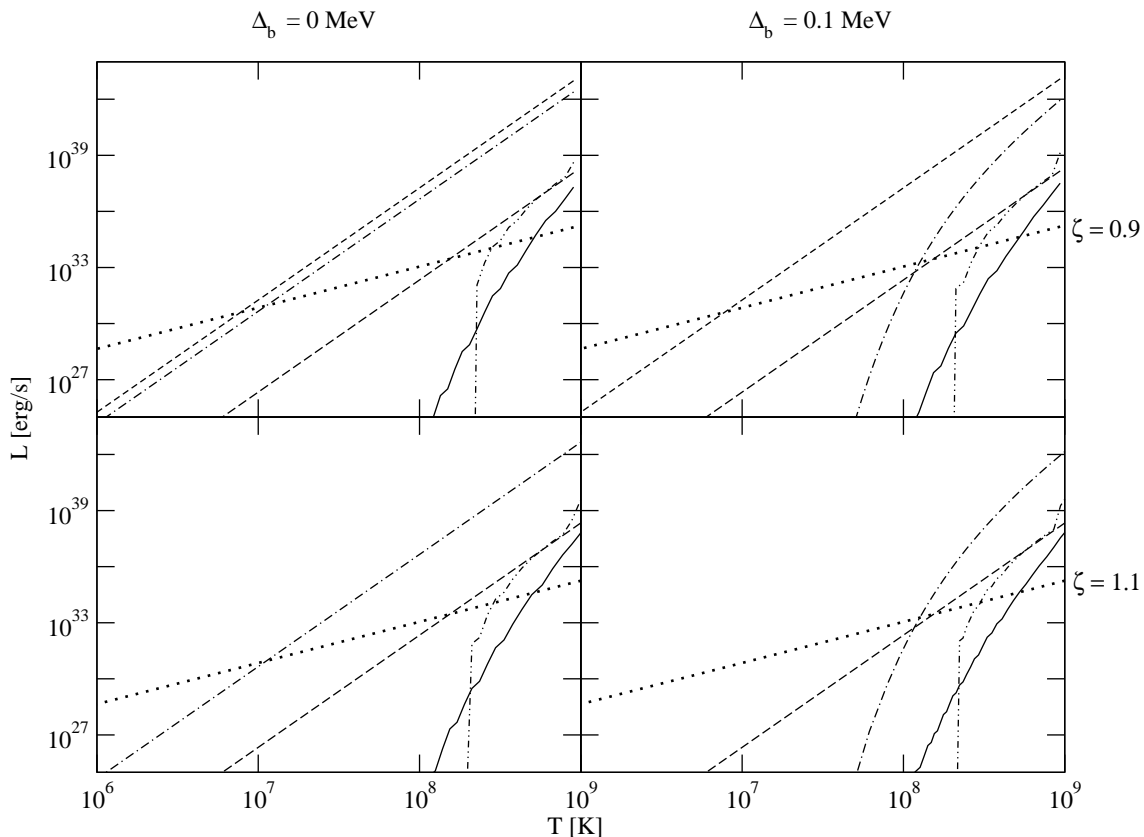


FIG. 4: Dependence of total luminosities of contributing processes on the core temperature: solid lines - Urca and bremsstrahlung processes in hadronic phase(s), long-dashed line - electron bremsstrahlung in the crusts, short dashed and dashed-dotted lines - Urca process with red-green and blue quarks, respectively, dashed-double-dotted lines - pair-breaking processes in the hadronic phases, dotted lines - photon emission from the surface. The underlying model corresponds to the 1.93 solar-mass model in Table I.

for the star model with central density  $\rho_{c,14} = 11.8$ . It is complementary to Fig. 3 in the sense that it allows us to identify the dominant cooling agent for each temperature and, hence, via Fig. 3, for each epoch. Clearly, the cooling mechanism with largest luminosity determines the rate of decrease of the temperature. Since no heating processes are included in our study, the asymptotic rate of the cooling is determined by the photon luminosity. The dominant cooling agent in the neutrino emission era depends on the microphysics input as explained in caption of Fig 4.

A general trend seen in each panel of Fig. 3 is that the heavier the star, the faster is its cooling by neutrinos. As a consequence, the heavy stars enter the photon cooling stage later than the lighter ones. In the late photon cooling era, the arrangement of the cooling curves is inverted, *i.e.*, the heavier stars are “hotter” than the lighter stars. (The photon luminosity of a star depends on its radius. Therefore, the heavier stars, which are more compact than the light ones, have smaller photon luminosities than the light stars of the same surface temperature; however, the cooling dynamics dominates over this static effect.) The fast cooling of massive stars in

the neutrino emission era is driven by the quark Urca process (see Fig. 4). Since the neutrino luminosity in Eq. (10) is an integral quantity, it scales with the size of the quark core  $L_\nu \propto [R^q]^3$ , and therefore increases with the size of the quark core. The scatter of cooling curves in the  $T - t$  plane suggests that the experimental data could be naturally accommodated in the models that have quark cores whose size changes as the central density of the model (and the net mass) are changed. In such an approach, the dichotomy in cooling behavior of neutron stars is attributed to the different masses of these objects: the lighter ones not containing quark matter cool more slowly than the heavier stars having quark cores. Note, however, that other factors, *e.g.*, surface magnetic fields or the envelope structure, could be responsible for differences observed in the surface temperatures of isolated neutron stars as well.

Superimposed on this general trend are the variations that arise from different functional dependence of the Urca emissivity of quarks on the temperature under different assumptions about the pairing pattern of quarks. We explore the variation of the parameters  $\Delta_b$  and  $\zeta$ . The fastest neutrino cooling occurs for  $\Delta_b = 0$  and  $\zeta = 0.9$

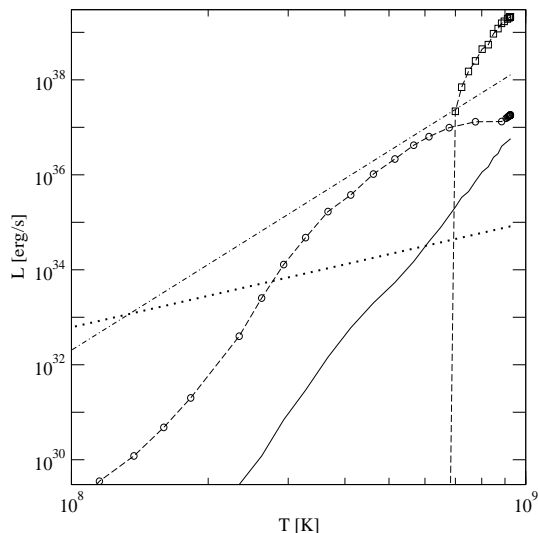


FIG. 5: Dependence of total luminosities on the core temperature for a  $1.1 M_{\odot}$  hadronic star. Solid line - the luminosity of two-nucleon processes (modified Urca and bremsstrahlung), dashed-dotted line - the bremsstrahlung luminosity in the crust, dotted line - the photon luminosity of the surface, circles - neutron pair-breaking process in the crust, squares - neutron and proton pair-breaking processes in the core.

(the upper left panels in Figs. 3 and 4). Indeed, in this case the Urca process is unsuppressed for all colors of quarks; the red-green quarks radiate neutrinos at rates comparable to unpaired quark matter, since there exist gapless excitations near the Fermi surfaces for  $\zeta < 1$ . The next-fastest cooling scenario corresponds to the choice  $\Delta_b = 0.1$  MeV and  $\zeta = 0.9$  (the upper right panel in Figs. 3 and Fig. 4); here, the contribution of blue quarks is suppressed for  $T < 10^9$  K, whereas the radiation from red-green quarks is unsuppressed as before. Therefore, the neutrino luminosity is reduced by about 1/3 from the case where all quark colors radiate at the rate of unpaired quark matter. The effect of a large blue-quark gap is clearly seen in Fig. 4 where the initially power-law drop of the luminosity with temperature changes to exponential. Let us turn to the case where red-green quarks are gapped over the entire Fermi surface, *i.e.*,  $\zeta > 1$ . Because their gap is substantially larger than the blue-quark gap, their neutrino luminosity is suppressed at a much larger temperature. (This corresponds to the case  $\zeta = 1.1$ , which is illustrated in the two panels in the lower row in Figs. 3 and 4.) In the case where  $\Delta_b = 0$  (lower left panel), we find the third-fastest neutrino-cooling scenario, in which the neutrino emission is dominated by the blue quarks and is about 30% of the rate that would be emitted by quarks of all colors. Finally, the slowest cooling scenario emerges when  $\Delta_b = 0.1$  MeV and  $\zeta = 1.1$  (lower right panel). The neutrino emission of quarks of all colors is shut off below the critical temperature of blue quarks. The photon cooling from the surface and the bremsstrahlung in the crust are dominant close to this

temperature, but the photon luminosity takes over as the temperature drops slightly further (see Fig. 4, lower left panel).

Figure 4 offers some further insight into the relative importance of various cooling processes. Specifically, the neutrino emission from the hadronic core with  $L_{core} \propto T^8$  in the unpaired matter is an unimportant source of cooling except in the slow cooling model, because of the exponential suppression due to the gaps in neutron and proton quasiparticle spectra. The bremsstrahlung process in the crusts with  $L_{crust} \propto T^6$  is numerically unimportant except for a limited range of temperatures prior to the transition to the photon cooling era. The fact that over long periods of time a single cooling process is dominant allows one to deduce the slope of the cooling curves, provided the specific heat capacity of the fermions scales linearly with temperature  $c_V = aT$  and the nontrivial temperature dependence arising from pairing effects can be neglected. Writing the luminosity of a process as  $L = bT^{n+2}$ , Eq. (10) can be integrated to obtain

$$t = t_0 + \frac{a}{bn} T(t)^{-n} \left( 1 - \frac{T(t)^n}{T_0^n} \right), \quad (11)$$

where  $t_0$  is the initial time and  $T_0 = T(t_0)$  is the initial temperature. The expression in the braces is unity for  $T(t) \ll T_0$ , so one finds the scaling  $t \sim T^{-n}$ . Thus, the neutrino-cooling time via quark Urca process scales as  $T^{-4}$ , while the cooling time via photons scales as  $T^{-1/5}$  for the surface-core temperature relation adopted above.

It is further instructive to examine the relative importance of different hadronic processes in a purely hadronic  $1.1 M_{\odot}$  mass star. As seen in Fig. 5, in the temperature domain  $7 \times 10^8 \leq T \leq T_c$  the neutrinos are produced predominantly by the pair-breaking processes in the core. At lower temperatures the crust electron bremsstrahlung and, to some extent, the pair-breaking bremsstrahlung in the crustal superfluid are the dominant processes. At about  $T \sim 10^8$  K the neutrino emission era ends and the photon cooling from the surface of the star becomes the dominant cooling process.

A comparison with the measured temperatures of neutron stars suggests that slow cooling models ( $\Delta_b = 0.1$  and  $\zeta = 1.1$ ) describe young, cool objects. The temperatures of the fast cooling models are well below the current measurements and upper limits. Our  $1.1 M_{\odot}$  hadronic model fails to account for the data on old and hot stars. There are several physical factors that may influence this outcome: (i) the rates of the neutrino bremsstrahlung of electrons in the crust may be overestimated due to the our assumption that the ions form a fluid [49]; (ii) if the crust bremsstrahlung is subdominant due to crystalline nature of the lattice, the pair-breaking process are the most important cooling agents in a wider temperature range and these depend sensitively on the values of not-well-constrained pairing gaps in the baryonic matter; (iii) variations in the magnetic fields and the surface composition of the neutron stars.



#### IV. CONCLUSIONS

Motivated partly by the recent observation of a massive compact object in a binary system [5] and partly by the recent development of sequences of stable massive hybrid stars with realistic input equations of state [24, 25], we have modeled the thermal evolution of compact stars containing quark cores. These sequences of stable stars allow for a transition from hadronic to quark matter in massive stars ( $M > 1.85M_{\odot}$ ) with the maximal mass of the sequence  $\sim 2M_{\odot}$ .

Our study has concentrated on the changes in the cooling behavior of the compact objects as the central density (and therefore macro-parameters such as the mass) is varied in a wide range along a sequence which has low-mass ( $M \leq 1.85M_{\odot}$ ) purely hadronic members and high-mass ( $M > 1.85M_{\odot}$ ) stars containing quark cores. We have seen that different cooling scenarios arise depending on the assumption of the magnitude of the pairing gaps in quark matter, including the possibility of emergence of a gapless phase in  $u$ - $d$  condensate of quarks.

We find that (i) the neutrino-cooling is slow for hadronic stars and becomes increasingly fast with an increase of the size of the quark core, in those scenarios where there are unpaired quarks or gapless excitations in the superconducting quark phase. The temperature scatter of the cooling curves in the neutrino cooling era is significant and can explain the observed variations in the surface temperature data of same age neutron stars. (ii) If quarks of all colors have gapped Fermi surfaces, the neutrino cooling shuts off early, below the pairing temperature of blue quarks; in this case, the temperature spread of the cooling curves is not as significant as in the fast cooling scenarios. (iii) As the stars evolve into the photon cooling stage the temperature distribution is inverted, *i.e.*, those stars that were cooler in the neutrino-cooling era are hotter during the photon cooling stage.

Before closing, we briefly state some potential modifications to the results above and some further refinements of the models presented above. In this work, we concentrated on the phase with two-flavor pairing. If the in-medium masses of strange quarks are low, they could appear at low densities relevant to compact stars; the cooling of objects containing condensates with strange quarks

has been studied elsewhere [28]. Since the fermionic excitations in these denser phases differ from those in our model, their cooling significantly differs from the cooling behavior we observe.

The late-time evolution of compact objects will be affected by the heating in their interiors, as indicated in Eq. (10). Heating processes change the thermal history in the photon cooling, implying a less steeper than  $\propto T^{-1/5}$  slope of temperature decay with time [58, 59]. While important, these processes are unlikely to affect the present results and conclusion, which are mainly concerned with the neutrino emission era.

Although our models have realistic density profiles derived from microscopic equations of state, we have assumed constant pairing gaps throughout the color superconducting phases. This is not the case, since the density of states at the Fermi surface and running coupling of strong interactions (both of which control the strength of pairing interactions) vary with density. As the density increases, the density of states increases as  $1/3$  power of density, whereas the strong coupling constant decreases logarithmically. These variations would be of minor importance unless the  $\zeta$  function occurs to cross  $\zeta = 1$  boundary separating the gapless and gapped phases. If this occurs, the core shell where  $\zeta < 1$  will be the predominant neutrino emitter; physically, instead of the entire core volume the effective radiation volume will amount to that of the shell where  $\zeta < 1$ . For any given model, this will reduce the neutrino luminosity of red-green quarks. A density-dependent  $\zeta$  parameter, combined with other parameters discussed above, can be used to fine-tune the models to fit the observational data. In particular, our models can be applied to describe the recently observed cooling behavior of the neutron star Cassiopeia A [60, 61].

#### Acknowledgments

We thank M. Alford, D. B. Blaschke, J. W. Clark, X.-G. Huang, B. Knippel, L. Rezzolla, D. H. Rischke, A. Schmitt, K. Schwenzer, and I. Shovkovy for useful discussions and B. Knippel for collaboration at the initial stages of this project.

- 
- [1] G. Glen and P. Sutherland, “On The Cooling of Neutron Stars,” *Astrophys. J.* **239**, 671 (1980).
- [2] D. Page, U. Geppert and F. Weber, “The Cooling of Compact Stars,” *Nucl. Phys. A* **777**, 497 (2006) [arXiv:astro-ph/0508056].
- [3] D. G. Yakovlev, O. Y. Gnedin, A. D. Kaminker and A. Y. Potekhin, “Theory of cooling neutron stars versus observations,” *AIP Conf. Proc.* **983**, 379 (2008) [arXiv:0710.2047 [astro-ph]].
- [4] A. Sedrakian, “The physics of dense hadronic matter and compact stars,” *Prog. Part. Nucl. Phys.* **58**, 168 (2007) [arXiv:nucl-th/0601086].
- [5] P. B. Demorest, T. Pennucci, S. M. Ransom, M. S. E. Roberts and J. W. T. Hessels, “A two-solar-mass neutron star measured using Shapiro delay,” *Nature* **467**, 1081 (2010).
- [6] K. Rajagopal and F. Wilczek, “The condensed matter physics of QCD,” arXiv:hep-ph/0011333.
- [7] M. G. Alford, “Color superconducting quark matter,” *Ann. Rev. Nucl. Part. Sci.* **51**, 131 (2001)

- [arXiv:hep-ph/0102047].
- [8] D. K. Hong, “Aspects of color superconductivity,” *Acta Phys. Polon. B* **32**, 1253 (2001) [arXiv:hep-ph/0101025].
- [9] D. H. Rischke, “The quark-gluon plasma in equilibrium,” *Prog. Part. Nucl. Phys.* **52**, 197 (2004) [arXiv:nucl-th/0305030].
- [10] I. A. Shovkovy, “Two lectures on color superconductivity,” *Found. Phys.* **35**, 1309 (2005) [arXiv:nucl-th/0410091].
- [11] M. G. Alford, A. Schmitt, K. Rajagopal and T. Schafer, “Color superconductivity in dense quark matter,” *Rev. Mod. Phys.* **80**, 1455 (2008) [arXiv:0709.4635 [hep-ph]].
- [12] Q. Wang, “Some aspects of color superconductivity: an introduction,” *Prog. Phys.* **30**, 173 (2010) [arXiv:0912.2485 [nucl-th]].
- [13] M. G. Alford, J. A. Bowers and K. Rajagopal, “Crystalline color superconductivity,” *Phys. Rev. D* **63**, 074016 (2001) [arXiv:hep-ph/0008208].
- [14] J. A. Bowers and K. Rajagopal, “The crystallography of color superconductivity,” *Phys. Rev. D* **66**, 065002 (2002) [arXiv:hep-ph/0204079].
- [15] H. M<sup>u</sup>ther and A. Sedrakian, “Breaking rotational symmetry in two-flavor color superconductors,” *Phys. Rev. D* **67**, 085024 (2003) [arXiv:hep-ph/0212317].
- [16] O. Kiriya, D. H. Rischke and I. A. Shovkovy, “Gluonic phase versus LOFF phase in two-flavor quark matter,” *Phys. Lett. B* **643**, 331 (2006) [arXiv:hep-ph/0606030].
- [17] R. Casalbuoni, R. Gatto, N. Ippolito, G. Nardulli and M. Ruggieri, “Ginzburg-Landau approach to the three flavor LOFF phase of QCD,” *Phys. Lett. B* **627**, 89 (2005) [Erratum-ibid. B **634**, 565 (2006)] [arXiv:hep-ph/0507247].
- [18] M. Mannarelli, K. Rajagopal and R. Sharma, “Rigid Crystalline Color-Superconducting Quark Matter,” *Prog. Theor. Phys. Suppl.* **174**, 39 (2008).
- [19] L. He, M. Jin and P. Zhuang, “Neutral Color Superconductivity Including Inhomogeneous Phases at Finite Temperature,” *Phys. Rev. D* **75**, 036003 (2007) [arXiv:hep-ph/0610121].
- [20] A. Sedrakian and D. H. Rischke, “Phase diagram of chiral quark matter: Fulde-Ferrell pairing from weak to strong coupling,” *Phys. Rev. D* **80**, 074022 (2009) [arXiv:0907.1260 [nucl-th]].
- [21] X. G. Huang and A. Sedrakian, “Phase diagram of chiral quark matter: color and electrically neutral Fulde-Ferrell phase,” *Phys. Rev. D* **82**, 045029 (2010) [arXiv:1006.0147 [nucl-th]].
- [22] M. Huang and I. A. Shovkovy, “Chromomagnetic instability in dense quark matter,” *Phys. Rev. D* **70**, 051501 (2004) [arXiv:hep-ph/0407049].
- [23] A. Sedrakian, H. M<sup>u</sup>ther and A. Polls, “Anomalous specific heat jump in a two-component ultracold Fermi gas,” *Phys. Rev. Lett.* **97**, 140404 (2006) [arXiv:cond-mat/0605085].
- [24] N. Ippolito, M. Ruggieri, D. Rischke, A. Sedrakian and F. Weber, “Equilibrium sequences of non rotating and rapidly rotating crystalline color-superconducting hybrid stars,” *Phys. Rev. D* **77**, 023004 (2008) [arXiv:0710.3874 [astro-ph]].
- [25] B. Knippel and A. Sedrakian, “Gravitational radiation from crystalline color-superconducting hybrid stars,” *Phys. Rev. D* **79**, 083007 (2009) [arXiv:0901.4637 [astro-ph.SR]].
- [26] D. Page, M. Prakash, J. M. Lattimer and A. Steiner, “Prospects of detecting baryon and quark superfluidity from cooling neutron stars,” *Phys. Rev. Lett.* **85**, 2048 (2000) [arXiv:hep-ph/0005094].
- [27] D. Blaschke, H. Grigorian and D. N. Voskresensky, “Cooling of hybrid neutron stars and hypothetical self-bound objects with superconducting quark cores,” *Astron. Astrophys.* **368**, 561 (2001) [arXiv:astro-ph/0009120].
- [28] M. Alford, P. Jotwani, C. Kouvaris, J. Kundu and K. Rajagopal, “Astrophysical implications of gapless color-flavor locked quark matter: A hot water bottle for aging neutron stars,” *Phys. Rev. D* **71**, 114011 (2005) [arXiv:astro-ph/0411560].
- [29] R. Anglani, G. Nardulli, M. Ruggieri and M. Mannarelli, “Neutrino emission from compact stars and inhomogeneous color superconductivity,” *Phys. Rev. D* **74**, 074005 (2006) [arXiv:hep-ph/0607341].
- [30] H. Grigorian, D. Blaschke and D. Voskresensky, “Cooling of neutron stars with color superconducting quark cores,” *Phys. Rev. C* **71**, 045801 (2005) [arXiv:astro-ph/0411619].
- [31] D. Blaschke and H. Grigorian, “Unmasking neutron star interiors using cooling simulations,” *Prog. Part. Nucl. Phys.* **59**, 139 (2007) [arXiv:astro-ph/0612092].
- [32] M. G. Alford, J. A. Bowers, J. M. Cheyne and G. A. Cowan, “Single color and single flavor color superconductivity,” *Phys. Rev. D* **67**, 054018 (2003) [arXiv:hep-ph/0210106].
- [33] M. Buballa, J. Hosek and M. Oertel, “Anisotropic admixture in color superconducting quark matter,” *Phys. Rev. Lett.* **90**, 182002 (2003) [arXiv:hep-ph/0204275].
- [34] A. Schmitt, “The ground state in a spin-one color superconductor,” *Phys. Rev. D* **71**, 054016 (2005) [arXiv:nucl-th/0412033].
- [35] A. Schmitt, I. A. Shovkovy and Q. Wang, “Neutrino emission and cooling rates of spin-one color superconductors,” *Phys. Rev. D* **73**, 034012 (2006) [arXiv:hep-ph/0510347].
- [36] P. Jaikumar, C. D. Roberts and A. Sedrakian, “Direct Urca neutrino rate in colour superconducting quark matter,” *Phys. Rev. C* **73**, 042801 (2006) [arXiv:nucl-th/0509093].
- [37] B. Knippel, “Color superconducting hybrid stars: structure, cooling, and gravitational waves”, Master Thesis, Frankfurt University, 2010.
- [38] A. Sedrakian, “Astrophysics of dense quark matter in compact stars,” *Acta Phys. Polon. B* **3**, 669 (2010) [arXiv:0910.4451 [astro-ph.SR]].
- [39] A. Sedrakian, “Cold quark matter in astrophysics of compact stars,” *AIP Conf. Proc.* **1317**, 372 (2011) [arXiv:1009.3826 [astro-ph.HE]].
- [40] N. Iwamoto, “Quark Beta Decay And The Cooling Of Neutron Stars,” *Phys. Rev. Lett.* **44**, 1637 (1980).
- [41] T. Schafer and K. Schwenzer, “Neutrino emission from ungapped quark matter,” *Phys. Rev. D* **70**, 114037 (2004) [arXiv:astro-ph/0410395].
- [42] A. Sedrakian, “Direct Urca neutrino radiation from superfluid baryonic matter,” *Phys. Lett. B* **607**, 27 (2005) [arXiv:nucl-th/0411061].
- [43] B. M<sup>u</sup>hlschlegel, “Die Thermodynamische Funktionen des Supraleiters,” *Zeit. für Physik* **155**, 313 (1959).
- [44] K. P. Levenfish and D. G. Yakovlev, *Astronomy Reports* **38**, 247 (1994).
- [45] Anomalous temperature dependence in unpaired quark

- matter can arise from non-Fermi liquid corrections due to finite range interactions, which are neglected here; see A. Ipp, A. Gerhold and A. Rebhan, “Anomalous specific heat in high density QED and QCD,” *Phys. Rev. D* **69**, 011901 (2004) [arXiv:hep-ph/0309019].
- [46] B. Friman and O. V. Maxwell, *Astrophys. J.* **232**, 541 (1979).
- [47] C. Schaab, D. Voskresensky, A. D. Sedrakian, F. Weber and M. K. Weigel, “Impact of medium effects on the cooling of non-superfluid and superfluid neutron stars,” *Astron. Astrophys.* **321**, 591 (1997) [arXiv:astro-ph/9605188].
- [48] G. G. Festa and M. A. Ruderman, *Phys. Rev.* **180**, 1227 (1969).
- [49] A. D. Kaminker, C. J. Pethick, A. Y. Potekhin, V. Thorsson and D. G. Yakovlev, *Astron. and Astrophys.* **343**, 1009 (1999).
- [50] E. Flowers, M. Ruderman and P. Sutherland, “Neutrino pair emission from finite-temperature neutron superfluid and the cooling of young neutron stars,” *Astrophys. J.* **205**, 541 (1976).
- [51] L. B. Leinson and A. Perez, “Vector current conservation and neutrino emission from singlet-paired baryons in neutron stars,” *Phys. Lett. B* **638**, 114 (2006) [arXiv:astro-ph/0606651].
- [52] A. Sedrakian, H. Muther and P. Schuck, “Vertex renormalization in weak decays of Cooper pairs and cooling compact stars,” *Phys. Rev. C* **76**, 055805 (2007) [arXiv:astro-ph/0611676].
- [53] E. E. Kolomeitsev and D. N. Voskresensky, “Neutrino emission due to Cooper-pair recombination in neutron stars revisited,” *Phys. Rev. C* **77**, 065808 (2008) [arXiv:0802.1404 [nucl-th]].
- [54] A. W. Steiner and S. Reddy, “Superfluid Response and the Neutrino Emissivity of Neutron Matter,” *Phys. Rev. C* **79**, 015802 (2009) [arXiv:0804.0593 [nucl-th]].
- [55] E. H. Gudmundsson, C. J. Pethick, and R. I. Epstein, “Structure of neutron star envelopes,” *Astrophys. J.* **272**, 286 (1983).
- [56] A. Y. Potekhin, G. Chabrier and D. G. Yakovlev, “Internal temperatures and cooling of neutron stars with accreted envelopes,” *Astron. Astrophys.* **323**, 415 (1997).
- [57] A. Y. Potekhin and D. G. Yakovlev, “Thermal structure and cooling of neutron stars with magnetized envelopes,” *Astron. Astrophys.* **374**, 213 (2001).
- [58] C. Schaab, A. Sedrakian, F. Weber and M. K. Weigel, “Impact of internal heating on the thermal evolution of neutron stars,” *Astron. Astrophys.* **346**, 465 (1999) [arXiv:astro-ph/9904127].
- [59] D. Gonzalez and A. Reisenegger, “Internal Heating of Old Neutron Stars: Contrasting Different Mechanisms,” arXiv:1005.5699 [astro-ph.HE].
- [60] C. O. Heinke and W. C. G. Ho, “Direct Observation of the Cooling of the Cassiopeia A Neutron Star,” *Astrophys. J.* **719**, L167 (2010) [arXiv:1007.4719 [astro-ph.HE]].
- [61] P. S. Shternin, D. G. Yakovlev, C. O. Heinke, W. C. G. Ho and D. J. Patnaude, *Mon. Not. Roy. Astron. Soc.* **412**, L108 (2011) [arXiv:1012.0045 [astro-ph.SR]].
- [62] J. Wambach, T. L. Ainsworth and D. Pines, “Quasiparticle interactions in neutron matter for applications in neutron stars,” *Nucl. Phys. A* **555**, 128 (1993).
- [63] M. Baldo, O. Elgaroey, L. Engvik, M. Hjorth-Jensen and H. J. Schulze, “Triplet P-3(2) to F-3(2) pairing in neutron matter with modern nucleon-nucleon potentials,” *Phys. Rev. C* **58**, 1921 (1998).
- [64] M. Baldo, J. Cugnon, A. Lejeune, U. Lombardo, “Neutron and proton superfluidity in neutron star matter,” *Nucl. Phys. A* **536**, 349 (1992).
- [65] D. Page, J. M. Lattimer, M. Prakash and A. W. Steiner, “Neutrino Emission from Cooper Pairs and Minimal Cooling of Neutron Stars,” *Astrophys. J.* **707**, 1131 (2009) [arXiv:0906.1621 [astro-ph.SR]]; D. Page, J. M. Lattimer, M. Prakash and A. W. Steiner, “Minimal cooling of neutron stars: a new paradigm,” *Astrophys. J. Suppl.* **155**, 623 (2004).
- [66] P. Slane, D. J. Helfand, E. van der Swaluw and S. S. Murray, *Astrophys. J.* **616**, 403 (2004) [arXiv:astro-ph/0405380].
- [67] J. P. Hughes, P. O. Slane, S. W. Park, P. W. A. Roming and D. N. Burrows, *Astrophys. J.* **591**, L139 (2003) [arXiv:astro-ph/0305383].
- [68] D. L. Kaplan, D. A. Frail, B. M. Gaensler, E. V. Gotthelf, S. R. Kulkarni, P. O. Slane and A. Nechita, arXiv:astro-ph/0403313.
- [69] J. P. Halpern, E. V. Gotthelf, F. Camilo, D. J. Helfand and S. M. Ransom, *Astrophys. J.* **612**, 398 (2004) [arXiv:astro-ph/0404312].